CrystEngComm

Accepted Manuscript

ROYAL SOCIETY OF CHEMISTRY

www.rsc.org/crystengcomm

CrystEngComm

Dynamic Article Links ►

Cite this: DOI: 10.1039/c4ce00000x

www.rsc.org/CrystEngComm

ARTICLE

Syntheses, Topologies, and Luminescence of Four Ln-Organic Polymers Constructed From Aromatic Tetracarboxylic Acids

Liming Fan,[a,b] Weiliu Fan,[a] Weikuo Song,[b] Guangzeng Liu,[b] Xiutang Zhang,*[a,b] Xian Zhao*[a]

Received (in XXX, XXX) Xth XXXXXXXXX 2014, Accepted Xth XXXXXXXXX 2014

DOI: 10.1039/c4ce00000x

ABSTRACT: Four new coordination polymers (CPs), $\{[H_2N(CH_3)_2]_2[Ln_2(BPT)(ox)_2]\}_n$ (Ln = Er for **1**, Yb for **2**, Sm for **3**, H_2ox = Oxalic acid) and $\{[Gd(HDCP)(H_2O)]\cdot H_2O\}_n$ (**4**), have been constructed from Ln ions and two aromatic tetracarboxylate acids (H_4BPT = 3,3',5,5'-biphenyltetracarboxylic acid, H_4DPT = 4,5-di(4'-carboxylphenyl)phthalic acid) under solvothermal reactions through the linker extension strategy. Their structures have been determined by single-crystal X-ray diffraction analyses and further characterized by elemental analyses, IR spectra, powder X-ray diffraction (PXRD), and thermogravimetric (TG) analyses. Complexes **1-3** are isomorphous and exhibit an unprecedented (6,8)-connected 3D architecture with the Point Symbol of $(3^3.4^{10}.5^7.6^2.7^6)(3^3.4^6.5^6)_2$, which is built up from right- and left-handed $[Ln(ox)]_n$ helixes. Complex **4** shows a 3D (4,8)-connected **flu** net with $(4^{12}.6^{12}.8^4)(4^6)_2$ topology based on 1D $[Gd(COO)_2]_n$ ladder chain. Moreover, their luminescent properties have been investigated.

Introduction

The coordination polymers (CPs), as an excellent representative of functional materials, have attracted upsurging research interest for their exceptional properties, such as, luminescence, NLO, magnetic, catalytic, gas storage and separation, drug delivery, and sensing.[1-3] Up to now, numerous CPs with structural diversity and topology novelty have been obtained, but rational design of those materials seemed difficult as not only reaction conditions but also building blocks have influences on the final structures.[4,5]

The lanthanide ions (Ln) based CPs holding unique advantages over other traditional CPs in those functional luminescent features, because the f–f transitions of lanthanide ions holding narrow bandwidth, high luminescence quantum yield, long-lived emission as well as large Stokes shift.[6-8] Besides, the introducing of organic ligands added the dimensional of those luminescent materials. Take the organic linkers and inorganic units into consideration, the Ln CPs provide special platforms for those functional materials.[9]

Recently, many polycarboxylates have been introduced into the Ln coordination frameworks by either ligand design or substituent modification.[10] Luminescence and other optical properties have been investigated in such materials. However, most of those Ln CPs are designed rather randomly and lack systematic comparison, which would be helpful to understand crystal growth and structure-property relationships.[11,12]

The 1,2,4,5-benzenetetracarboxylic acid (H_4BTC), as the most widely used aromatic tetracarboxylate, coorperated with Ln ions, have been constructed as much as 93 CPs with interesting structures and remarkable properties, proved by a CSD (Cambridge Structure Database) survey with the help of ConQuest version 1.3. As we all known, with the length increasing, the longer separation of neighboring Ln ions makes the organic ligands adopt more open coordination modes, and the obtained final structures tend to more complicated.[13] Such a linker extension strategy in the construction of Ln CPs inspires us to go further. With the H_4BTC expanded along different directions, two similar aromatic tetracarboxylate (H_4BPT = 3,3',5,5'-biphenyltetracarboxylic acid, H_4DPT = 4,5-di(4'-carboxylphenyl)phthalic acid) were selected to assemble polymeric complexes under solvothermal conditions.

Herein, we reported the syntheses and characterizations of four novel Ln CPs constructed from Ln ions and two aromatic tetracarboxylate acids through the linker extension strategy (Scheme 1), $\{[H_2N(CH_3)_2]_2[Ln_2(BPT)(ox)_2]\}_n$ (Ln = Er for **1**, Yb for **2**, and Sm for **3**) and $\{[Gd(HDCP)(H_2O)]\cdot H_2O\}_n$ (**4**). Interestingly, the structure analyses reveal that complexes **1-3** are isomorphous and exhibit an unprecedented (6,8)-connected 3D architecture with the Point Symbol of $(3^3.4^{10}.5^7.6^2.7^6)(3^3.4^6.5^6)_2$, which is built up from right- and left-handed $[Ln(ox)]_n$ helixes. Complex **4** shows a 3D (4,8)-connected **flu** net with $(4^{12}.6^{12}.8^4)(4^6)_2$ topology based on a $[Gd(COO)_2]_n$ ladder chain. Moreover, luminescent properties of complexes **1**–**4** have been studied.

---

[a] *State Key Laboratory of Crystal Materials, Shandong University , Jinan 250100, China.*
E-mail: zhaoxian@icm.sdu.edu.cn.
[b] *Advanced Material Institute of Research, College of Chemistry and Chemical Engineering, Qilu Normal University, Jinan, 250013, China.*
E-mail: *xiutangzhang@163.com.*

† Electronic Supplementary Information (ESI) available: Additional Figures, powder X-ray diffraction (PXRD) patterns, thermogravimetric analysis (TGA) and IR spectra for **1**–**4**. X-ray crystallographic data, CCDC 1003789–1003792 for **1**–**4**. See DOI:10.1039/c4ce00000x.

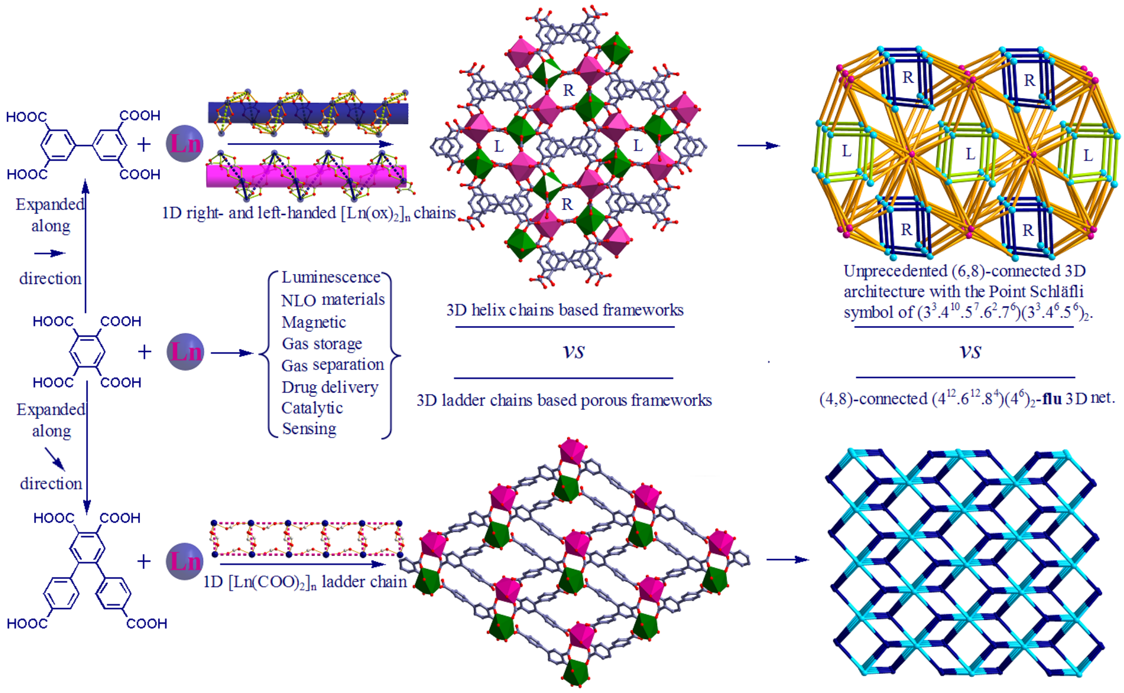

Scheme 1. Linker extension strategy in aromatic tetracarboxylate based Ln coordination polymers.

Experimental Section

Materials and Physical Measurements. All chemicals were purchased from Jinan Henghua Sci. & Tec. Co. Ltd. without further purification. IR spectra were measured on a NEXUS 670 FTIR spectrometer at the range of 600-4000 cm^{-1}. Elemental analyses were carried out on a CE instruments EA 1110 elemental analyzer. X-ray powder diffractions were measured on a Panalytical X-Pert pro diffractometer with Cu-Kα radiation. Thermogravimetric analyses (TGA) were performed under air condition from room temperature to 800 °C with a heating rate of 10 °C min^{-1} on Perkin-Elmer TGA-7 thermogravimetric analyzer. Fluorescence spectra were performed on a Hitachi F-4500 fluorescence spectrophotometer at room temperature.

Synthesis of $\{[H_2N(CH_3)_2]_2[Er_2(BPT)(ox)_2]\}_n$ (1). A mixture of H_4BPT (0.20 mmol, 0.066 g), $Er(OAc)_3\cdot 4H_2O$ (0.20 mmol, 0.075 g), oxalic acid (0.30mmol, 0.027g), NaOH (0.60 mmol, 0.024 g), 8 mL H_2O, 2 mL EtOH, and 2 mL DMF was placed in a Teflon-lined stainless steel vessel, heated to 170 °C for 3 days, followed by slow cooling (about 10 °C/h) to room temperature. The red block crystals of **1** were obtained. Yield of 59 % (based on Er). Anal. (%) calcd. for $C_{24}H_{20}Er_2O_{18}$(930.92): C, 30.96; H, 2.17. Found: C, 30.87; H, 2.25. IR (KBr pellet, cm^{-1}): 3389 (m), 3118 (m), 2803 (m), 1687 (m), 1604 (s), 1471 (s), 1415 (m), 1365 (s), 1316 (m), 1083 (w), 1018 (w), 791 (m), 711 (w).

Synthesis of $\{[H_2N(CH_3)_2]_2[Yb_2(BPT)(ox)_2]\}_n$ (2). The same synthetic procedure as for **1** was used except that $Er(OAc)_3\cdot 4H_2O$ was replaced by $Yb(NO_3)_3\cdot 6H_2O$ (0.20 mmol, 0.093 g), giving colorless block crystals. Yield of 54 % (based on Yb). Anal. (%) calcd. for $C_{24}H_{20}O_{18}Yb_2$ (942.48): C, 30.58; H, 2.14. Found: C, 29.82; H, 2.37. IR (KBr pellet, cm^{-1}): 3341 (m), 3058 (s), 2746 (m), 1699 (w), 1578 (s), 1542 (s), 1456 (m), 1424 (s), 1358 (s), 1108 (w), 1017 (m), 918 (w), 709 (w).

Synthesis of $\{[H_2N(CH_3)_2]_2[Sm_2(BPT)(ox)_2]\}_n$ (3). The same synthetic procedure as for **1** was used except that $Er(OAc)_3\cdot 4H_2O$ was replaced by $Sm(NO_3)_3\cdot 6H_2O$ (0.20 mmol, 0.089 g), giving colorless block crystals. Yield of 61 % (based on Sm). Anal. (%) calcd. for $C_{24}H_{20}O_{18}Sm_2$ (897.12): C, 32.13; H, 2.25. Found: C, 31.98; H, 2.41. IR (KBr pellet, cm^{-1}): 3436 (m), 3152 (m), 1704 (w), 1606 (vs), 1469 (s), 1423 (m), 1363 (s), 1314 (s), 1023 (w), 893 (w), 791 (m), 716 (w).

Synthesis of $\{[Gd(HDCP)(H_2O)]\cdot H_2O\}_n$ (4). A mixture of H_4DCP (0.10 mmol, 0.040 g), $GdCl_3\cdot 6H_2O$ (0.13 mmol, 0.050 g), NaOH (0.10 mmol, 0.004 g), and 14 mL H_2O was placed in a Teflon-lined stainless steel vessel, heated to 170 °C for 3 days, followed by slow cooling (a descent rate of 10 °C/h) to room temperature. Colorless block crystals of **4** were obtained. Yield of 47 % (based on Gd). Anal. (%) calcd. for $C_{44}H_{28}Gd_2O_{19}$ (1175.18): C, 44.97; H, 2.40. Found: C, 44.72; H, 2.43. IR (KBr pellet, cm^{-1}): 3457 (m), 3086 (m), 2636 (m), 1723 (m), 1693 (m), 1590 (s), 1520 (vs), 1411 (vs), 1181 (m), 864 (m), 788 (m), 721 (w).

X-ray Crystallography. Intensity data collection was carried out on a Siemens SMART diffractometer equipped with a CCD detector using Mo-*Kα* monochromatized radiation (λ = 0.71073 Å) at 296(2) or 293(2) K. The absorption correction was based on multiple and symmetry-equivalent reflections in the data set using the SADABS program based on the method of Blessing. The structures were solved by direct methods and refined by full-matrix least-squares using the SHELXTL package.[14] All non-hydrogen atoms were refined anisotropically. Hydrogen atoms were generated geometrically with fixed isotropic thermal parameters. Crystallographic data for complexes **1–4** are given in Table 1. Selected bond lengths and angles for **1–4** are listed in Table S1. For complexes of **1–4**, further details on the crystal structure investigations may be obtained from the Cambridge Crystallographic Data Centre, CCDC, 12 Union Road, CAMBRIDGE CB2 1EZ, UK, [Telephone:+44-(0)1223-762-910, Fax: +44-(0)1223-336-033; Email: deposit@ccdc.cam.ac.uk, http://www.ccdc.cam.ac.uk/deposit], on quoting the depository number CCDC–1003789 for **1**, 1003790 for **2**, 1003791 for **3**, and 1003792 for **4**. Topological analysis of the coordination networks of **1–4** was performed with the program package TOPOS.[15]

Result and Discussion

Synthesis and Characterization. Complexes **1-4** were obtained by the solvothermal reactions of H_4BPT or H_4DCT and related lanthanide salts. They are stable in the air and have poor solubility in water and common organic solvents but can be slightly soluble in very high polarity solvents.

Powder X-ray diffraction (PXRD) has been used to check the phase purity of the bulk samples in the solid state. For complexes **1−4**, the measured PXRD patterns closely match the simulated patterns generated from the results of single crystal diffraction data, indicative of pure products (Fig. S1, see Supporting Information). The absorption bands around 3400 cm^{-1} for **1-4** can be attributed to the characteristic peaks of O-H vibrations. The vibrations at ca. 1500 and 1610 cm^{-1} correspond to the asymmetric and symmetric stretching vibrations of the carboxyl groups, respectively (Fig. S2).

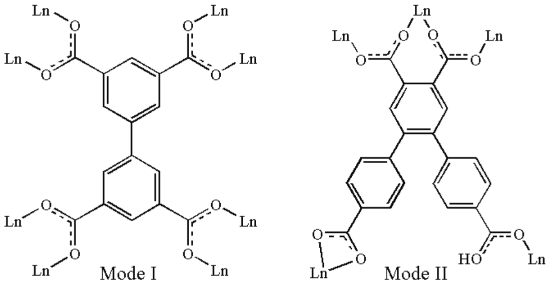

Scheme 2. The coordination modes of H_4BPT and H_4DCP in**1–4**.

Structure descriptions of $\{[H_2N(CH_3)_2]_2[Ln_2(BPT)(ox)_2]\}_n$ (Ln = Er for 1, Yb for 2, and Sm for 3). The single-crystal X-ray diffraction analyses reveal that complexes **1–3** are isomorphous and crystallize in the orthorhombic system, *P*na2(1) space group, herein only the structure of **1** will be discussed as a representation. As can be seen from Fig. 1, there are two Er^{III} ions, one completely deprotonated BPT^{4-} ligand, two ox^{2-} anions, and two dimethylammonium ions for charge balance. The coordination environments of two Er^{III} ions are similar, both coordinated with eight O atoms from four BPT^{4-} ligands and two ox^{2-} anions, with the Er–O bond distances range from 2.242(4) to 2.503(5) Å (Table. S1).

The BPT^{4-} ligand is completely deprotonated in complex **1** and linked with eight Er^{III} ions with four bridging μ_2-η^1:η^1 carboxyl groups (Mode I, Scheme 2), successfully assembly a 3D network with 1D void channels (Radius is about 5.32 Å) along *c* direction. The torsion dihedral angle between the two phenyl rings is 23.38(9)°, which indicates that the BPT^{4-} ligand is twisted to satisfy the coordination preference of Ln ions. Besides, it is interestingly to note that each ox^{2-} anion in complex **1** is coordinated with two neighbouring Er^{III} ions in a μ_2-bridging mode, giving 1D right- and left- handed $[Er(ox)]_n^{n-}$ helix chains with the diameter of the surrounding void channel is about 4.30 Å (Fig. 2). And the ox^{2-} anion separated Er···Er distances are 6.117 Å and 6.220 Å, respectively. As can be seen in Fig. 3, the 1D right- and left- handed $[Er(ox)]_n^{n-}$ helical chains alternately occupied the void channels of the 3D $[Er(BPT)]_n^{n-}$ networks, finally given an achiral 3D framework.

To better understand the whole structure of complex **1**, the topological analysis approach is employed. Each BPT^{4-} ligand connecting eight Er^{III} ions is defined as a eight-connected node, and each Er^{III} ion was linked by two ox^{2-} and four BPT^{4-} ligands, forming a 6-connected node. Thus, from the topological point of view, the final 3D framework can be regard as a binodal (6,8)-connected net with the Point Symbol of $(3^3.4^{10}.5^7.6^2.7^6)(3^3.4^6.5^6)_2$, shown in Fig.4.

Table 1 Crystal data for **1 – 5**.

Compound	**1**	**2**	**3**	**4**
Empirical formula	$C_{24}H_{22}Er_2N_2O_{16}$	$C_{24}H_{22}N_2O_{16}Yb_2$	$C_{24}H_{22}N_2O_{16}Sm_2$	$C_{22}H_{15}GdO_{10}$
Formula weight	928.96	940.52	895.14	596.59
Crystal system	Orthorhombic	Orthorhombic	Orthorhombic	Triclinic
Space group	*P*na2(1)	*P*na2(1)	*P*na2(1)	*P*-1
a (Å)	18.8991(14)	18.825(14)	19.116(7)	6.4355(12)
b (Å)	15.5229(11)	15.373(11)	15.714(6)	13.462(2)
c (Å)	9.0702(7)	9.047(7)	9.069(4)	13.753(2)
α (°)	90	90	90	61.532(2)
β (°)	90	90	90	82.433(3)
γ (°)	90	90	90	81.244(2)
V(Å^3)	2660.9(3)	2618(3)	2724.0(18)	1032.8(3)
Z	4	4	4	2
D_{calcd} (Mg/m^3)	2.319	2.386	2.183	1.918
μ(mm^{-1})	6.351	7.188	4.354	3.270
θ range (°)	1.70–25.00	2.16–25.00	2.13–25.00	1.77–25.00
Reflections collected	13143	12158	13500	5226
Data/Parameters	4494/402	4311/402	4715/402	3598/298
F(000)	1776	1792	1728	582
Flack	0(10)	0.00(3)	0.00(11)	N/A
T(K)	296(2)	296(2)	296(2)	293(2)
R_{int}	0.0268	0.0609	0.0374	0.0146
R_1 (wR_2) [$I > 2\sigma(I)$]	0.0228 (0.0543)	0.0376 (0.0614)	0.0282(0.0670)	0.0212 (0.0608)
R_1 (wR_2) (all data)	0.0233 (0.0546)	0.0403 (0.0621)	0.0297 (0.0676)	0.0217 (0.0611)
Gof	1.001	0.997	0.998	1.000

$R_1 = \Sigma| |F_o|-|F_c| |/ \Sigma|F_o|$, $wR_2 = [\Sigma w(F_o^2-F_c^2)^2]/ \Sigma w(F_o^2)^2]^{1/2}$

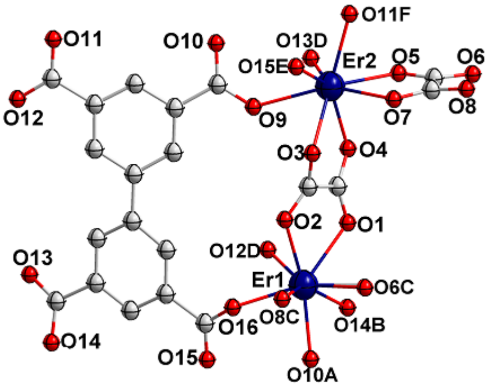

Figure 1. Perspective view of coordination environment of Er^{III} in **1** (Symmetry codes: A: *x*+1/2, -*y*+1/2, *z*; B: -*x*+1/2, *y*-1/2, *z*+1/2; C: -*x*, -*y*, *z*-1/2; D: -*x*, -*y*+1, *z*+1/2; E: *x*-1/2, -*y*+1/2, *z*; F: -*x*-1/2, *y*-1/2, *z*+1/2.).

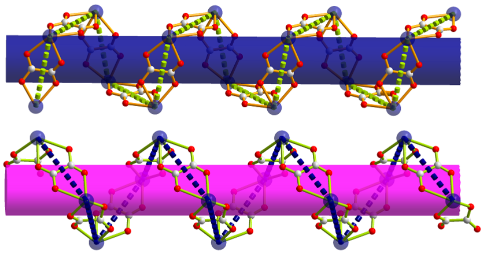

Figure 2. View of 1D right- and left- handed $[Er(ox)]_n^{n-}$ helical chains.

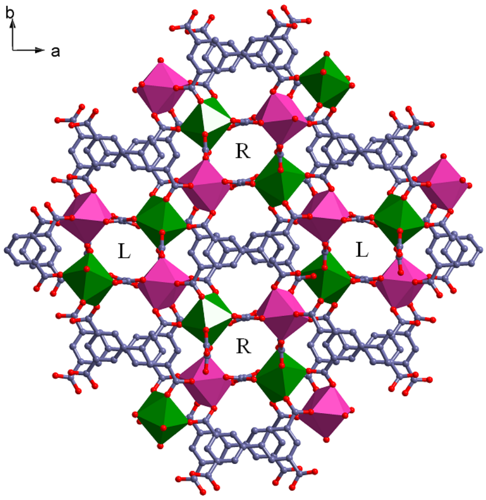

Figure 3. Schematic view of the 3D frameworks with right- and left-handed helical chains along *c* direction (green polyhedrons: Er(1) ions; red polyhedrons: Er(2) ions.).

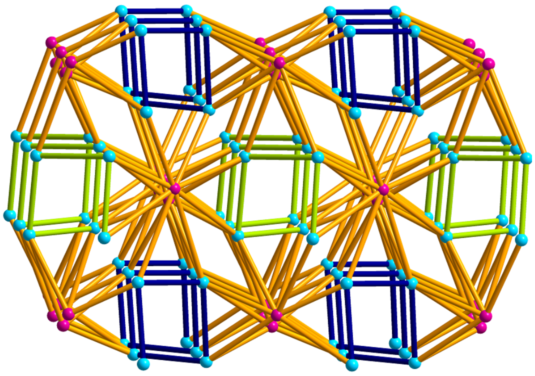

Figure 4. Views of the (6,8)-connected 3D architecture with unprecedented $(3^3.4^{10}.5^7.6^2.7^6)(3^3.4^6.5^6)_2$ topology (green spheres: Er^{III} ions; red spheres: BPT^{4-} ligands; grass green and blue bonds: ox^{2-} anions.).

Structure descriptions of $\{[Gd(HDCP)(H_2O)]\cdot H_2O\}_n$ (4). The X-ray single-crystal diffraction analysis reveals that complex **4** is a 3D framework and crystallizes in triclinic *P*-1 space group. The asymmetric unit of **4** contains one crystallographically independent Gd^{III} ion, one $HDCP^{3-}$ ligand, one coordinated water molecule, and one lattice water molecule. As shown in Fig. 5, Gd^{III} ion located in $\{GdO_8\}$ coordination environment, surrounded by eight oxygen atoms from five different $HDCP^{3-}$ ligands and one coordinated water molecule, exhibiting a slightly distorted square antiprism configuration. The Gd-O bond distances are in the range of 2.296(2) to 2.473(2) Å (Table. S1). The H_4DCP is partly deprotonated, and the four carboxyl groups showing three coordination types: bridging μ_2-η^1:η^1, cheating μ_1-η^1:η^1, and monodentating μ_1-η^1:η^0 (Mode II, Scheme 2). The dihedral angles among three phenyl rings are 52.76(3)°, 38.06(7)°, and 54.79(6)°, indicates the phenyl rings in $HDCP^{3-}$ have rotated through the C-C bonds to grip the neighbouring Gd^{III} ions.

Two neighbouring carboxyl groups in a same $HDCP^{3-}$ linked two symmetrical Gd^{III} ions to generate a dinuclear $\{Gd_2(COO)_4\}$ SBUs with Gd···Gd distance of 5.391 Å, and the SBUs are further extended into a 1D $[Gd(COO)_2]_n$ ladder chain by the bridging μ_2-η^1:η^1 carboxyl groups from other $HDCP^{3-}$ ligands (Fig. 6). Theμ_2-η^1:η^1 carboxyl groups separated Gd···Gd distance is 6.435 Å. Then each $HDCP^{3-}$ ligand linked with four 1D $[Gd(COO)_2]_n$ ladder chains, forming an interestingly 3D network along *bc* plane (Fig. 7). It is noteworthy that a rhombic channel with a 8.548 × 8.548 Å^2 opening area existed in the final framework, in which the lattice water molecules occupied. If the guest water molecules are omitted, calculation PLATON shows that the void volume of complex **4** is 5.4% of the crystal volume (55.4 out of the 1032.8 Å^3 unit cell volumes).[16] The low porosity can be attributed to the high coordination number of Ln^{III} ions.

From the viewpoint of structural topology, the $HDCP^{3-}$ ligand linked with four $\{Gd_2(COO)_4\}$ SBUs as 4-connected node, and the dinuclear $\{Gd_2(COO)_4\}$ SBUs act as 8-connected nodes, the whole 3D structure exhibits a binodal (4,8)-connected **flu** architecture with the Point Symbol of $(4^{12}.6^{12}.8^4)(4^6)_2$ (Fig. 8).

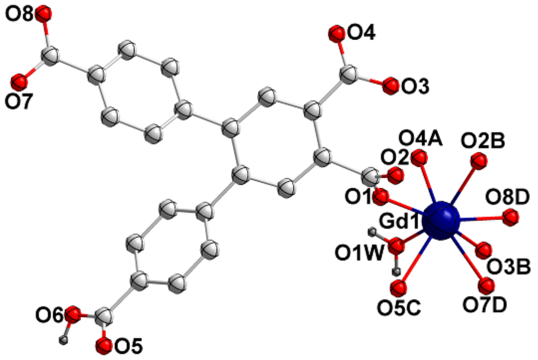

Figure 5. Coordination environment of Gd^{III} in **4** (Symmetry codes: A: -*x*+2, -*y*-1, -*z*+2; B: -*x*+1, -*y*-1, -*z*+2; C: -*x*+1, -*y*, -*z*+1; D: *x*-1, *y*-1, *z*.).

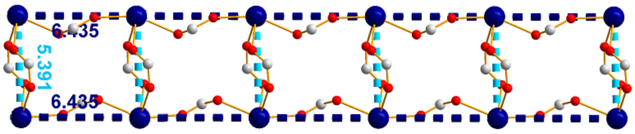

Figure 6. The 1D $[Gd(COO)_2]_n$ ladder chain in complex **4**.

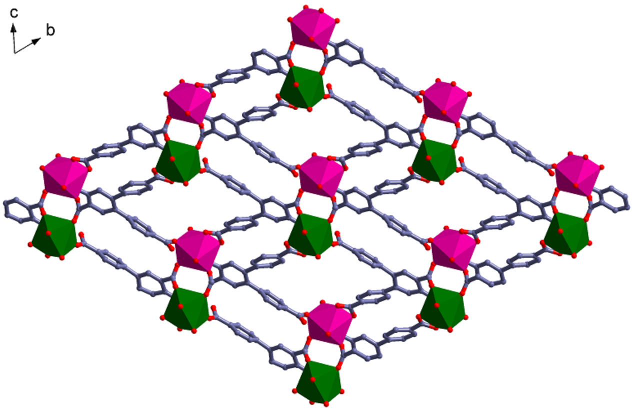

Figure 7. Schematic view of the self-penetrating like 3D frameworks in complex **4** along *a* direction.

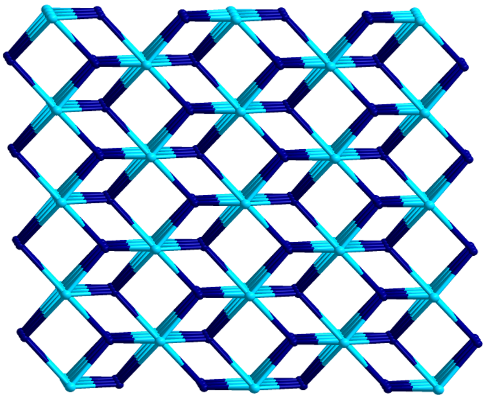

Figure 8. Views of the (4,8)-connected **flu** net with $(4^{12}.6^{12}.8^4)(4^6)_2$ topology (green spheres: $\{Gd_2(COO)_4\}$ SBUs; blue spheres: $HDCP^-$ ligands.).

Thermal Analyses. The experiments of thermogravimetric analysis (TGA) were performed on samples of **1-4** under N_2 atmosphere with a heating rate of 10 °C min^{-1}, shown in Fig. S5. Because of the isostructure of complex **1-3**, the three compounds exhibited similar thermal stability, the TG curve displays mainly two steps of weight loss processes.The first weight loss of 10.2 % (calc. 9.9 %) for **1**, 9.6 % (calc. 9.8 %) for **2**, and 9.7 % (calc. 10.3 %) for **3** occurred below 230 °C can be attributed to the loss of dimethylammoniumions. And then the organic ligands begin to collapse with a result of thermal decomposition. The TGA curve of **4** shows the initial weight loss below 160 °C, which can be ascribed to the removal of lattice water molecules as well as coordinated water molecules 5.9 % (calc. 6.0 %). Further weight loss observed above 430 °C indicates the decomposition of coordination framework.

Photoluminescent Investigation. The fluorescence spectrums of **1-4** and two free ligands were examined in the solid state at room temperature, shown in Fig. 9 and Fig. S6. The H_4BPT shows emission peak at 416 nm upon excitation at 346 nm, the H_4DCP displays emission peak at 407 nm upon excitation at 358 nm, both can be attributed to the π^*-π transition of the p electrons of the aromatic rings.[17] Complex **1** exhibits characteristic Er^{III} emissions (excited at 225 nm). The emission bands at 353, 371, 397, 419 nm arise from the $^4F_{9/2}\rightarrow{}^6I_{15/2}$, $^4F_{9/2}\rightarrow{}^6I_{13/2}$, $^4F_{9/2}\rightarrow{}^6I_{11/2}$, and $^4F_{9/2}\rightarrow{}^6I_{9/2}$ transitions, respectively.[18] For complex **2**, the emission bands at 402 nm is attributed to π^*-π transitions of $HBPT^{3-}$. Complex **3** displays the narrow and characteristic luminescence due to $^4G_{5/2}\rightarrow{}^6F_{11/2}$, $^4G_{5/2}\rightarrow{}^6F_{9/2}$, $^4G_{5/2}\rightarrow{}^6F_{7/2}$, and $^4G_{5/2}\rightarrow{}^6F_{5/2}$ transitions resulting from Sm^{III} ion, with the emission bands at 580, 426, 415, 396 nm (λ_{ex} = 303 nm).[19] For complex **4** , the emission bands at 405 nm upon excitation at 336 nm can be attributed to π^*-π transitions of $HDCP^{3-}$.

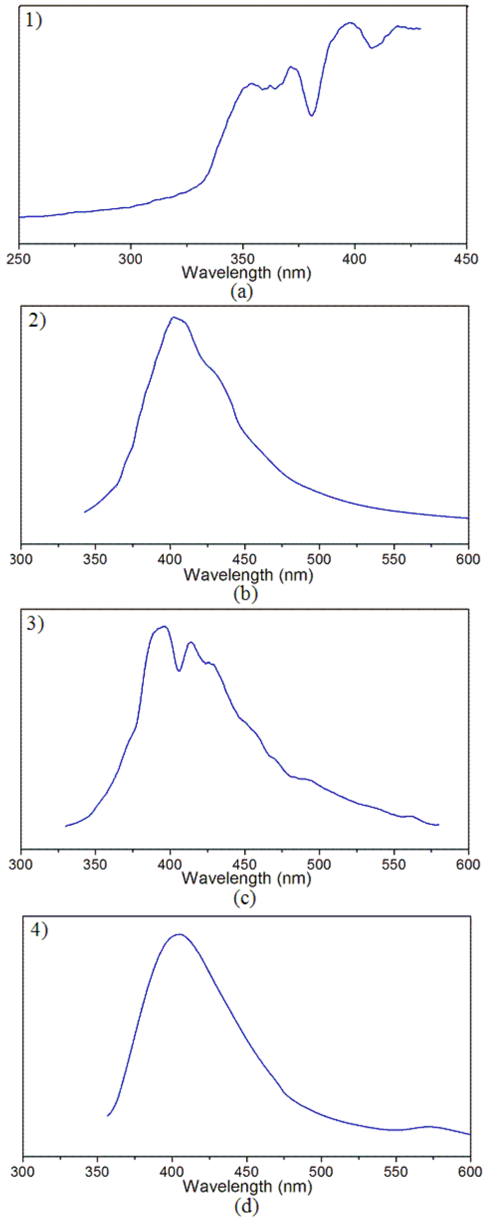

(a)

(b)

(c)

(d)

Figure 9. Emissionspectra of complexes **1-4** (a-d) in the solid state at room temperature.

Conclusions

In summary, four novel Ln coordination polymers based on tetracarboxylate acids have been hydrothermally synthesized through linker extension strategy. Complexes **1-3** are isomorphous and exhibit an unprecedented (6,8)-connected 3D $(3^3.4^{10}.5^7.6^2.7^6)(3^3.4^6.5^6)_2$ architecture with right- and left-handed $[Ln(ox)]_n$ helixes. Complex **4** shows a 3D (4,8)-connected **flu** net with $(3^{12}.6^{12}.8^4)(4^6)_2$ topology based on a $[Gd(COO)_2]_n$ ladder chain. These four luminescent functional CPs, based on helix or ladder chains, have significantly expanded the pool of inorganic building blocks and are clearly useful for the construction of functional luminescent CPs. Further work on the polycarboxylates based Ln CPs are underway in our lab.

Acknowledgements. The work was supported by financial support from the Natural Science Foundation of China (Grant Nos. 21101097, 91022034 and 51172127).

Notes

The authors declare no competing financial interest.

References

1. (a) M. O'Keeffe and O. M. Yaghi, *Chem. Rev.*, 2012, **112**, 675; (b) B. L. Chen, N. W. Ockwig, A. R. Millward, D. S. Contreras and O. M. Yaghi, *Angew. Chem. Int. Ed.*, 2005, **44**, 4745; (c) Y. Cui, Y. Yue, G. Qian and B. L. Chen, *Chem. Rev.*, 2012, **112**, 1126; (d) G. Férey and C. Serre, *Chem. Soc. Rev.*, 2009, **38**, 1380.
2. (a) M. Kim, J. F. Cahill, H. Fei, K. A. Prather and S. M. Cohen, *J. Am. Chem. Soc.*, 2012, **134**, 18082; (b) H. Fei, J. F. Cahill, K. A. Prather and S. M. Cohen, *Inorg. Chem.*, 2013, **52**, 4011; (c) P. V. Dau and S. M. Cohen, *Chem. Commun.*, 2013, **49**, 6128; (d) D. Sun, S. Yuan, H. Wang, H. F. Lu, S. Y. Feng and D. F. Sun, *Chem. Commun.*, 2013, **49**, 6152; (e) X. T. Zhang, L. M. Fan, X. Zhao, D. Sun, D. C. Li, J. M. Dou, *CrystEngComm*, 2012, **14**, 2053; (f) F. Guo, F. Wang, H. Yang, X. L. Zhang and J. Zhang, *Inorg. Chem.*, 2012, **51**, 9677; (g) K. Wang, S. Zeng, H. Wang, J. Dou and J. Jiang, *Inorg. Chem. Front.*, 2014, **1**, 167.
3. (a) H. Wang, K. Qian, D. Qi, W. Cao, K. Wang, S. Gao and J. Jiang, *Chem. Sci.*, 2014, **5**, 3214; (b) X. T. Zhang, D. Sun, B. Li, L. M. Fan, B. Li and P. H. Wei, *Cryst. Growth Des.*, 2012, **12**, 3845; (c) J. B. Lin, W. Xue, B. Y. Wang, J. Tao, W. X. Zhang, J. P. Zhang and X. M. Chen, *Inorg. Chem.*, 2012, **51**, 9423; (d) X. Zhang, L. Fan, W. Zhang, Y. Ding, W. Fan and X. Zhao, *Dalton. Trans.*, 2013, **42**, 16562; (e) Y. Zhang, W. Gao, K. Wang and J. Jiang, *Dalton Trans.*, 2014, **43**, 9152; (f) D. Zhang, W. Si, P. Wang, X. Chen and J. Jiang, *Inorg. Chem.*, 2014, **53**, 3494.
4. (a) D. X. Xue, J. B. Lin, J. P. Zhang and X. M. Chen, *CrystEngComm.*, 2009, **11**, 183; (b) X. Zhang, L. Fan, Z. Sun, W. Zhang, D. Li, J. Dou and L. Han, *Cryst. Growth Des.*, 2013, **13**, 792; (c) X. Zhang, L. Fan, W. Zhang, W. Fan and X. Zhao, *CrystEngComm*, 2014, **16**, 3203; (d) L. Fan, X. Zhang, W. Zhang, Y. Ding, W. Fan, L. Sun and X. Zhao, *CrystEngComm*, 2014, **16**, 2144; (e) H. Wang, C. Liu, T. Liu, S. Zeng, W. Cao, Q. Ma, C. Duan, J. Dou and J. Jiang, *Chem. Commun.*, 2013, **49**, 889; (f) L. Fan, Y. Gao, G. Liu, W. Fan, W. Song, L. Sun, X. Zhao and X. Zhang, *CrystEngComm*, 2014, **16**, 7649.
5. (a) A. H. Shelton, I. V. Sazanovich, J. A. Weinstein and M. D. Ward, *Chem. Comm.*, 2012, **48**, 2749; (b) L. Fan, X. Zhang, D. Li, D. Sun, W. Zhang and J. Dou, *CrystEngComm*, 2013, **15**, 349; (c) X. T. Zhang, L. M. Fan, X. Zhao, D. Sun, D. C. Li, J. M. Dou, *CrystEngComm*, 2012, **14**, 2053; (d) L. Fan, X. Zhang, Z. Sun, W. Zhang, Y. Ding, W. Fan, L. Sun, X. Zhao and H. Lei, *Cryst. Growth Des.*, 2013, **13**, 2462; (e) L. Fan, X. Zhang, W. Zhang, Y. Ding, W. Fan, L. Sun, Y. Pang and X. Zhao, *Dalton. Trans.*, 2014, **43**, 6701; (f) X. Zhang, L. Fan, W. Song, W. Fan, L. Sun and X. Zhao, *RSC Adv.*, 2014, **4**, 30274.
6. (a) Z. Y. Guo, H. Wu, G. Srinivas, Y. M. Zhou, S. C. Xiang, Z. X. Chen, Y. T. Yang, W. Zhou, M. O'Keeffe and B. L. Chen, *Angew. Chem., Int. Ed.*, 2011, **50**, 3178; (b) X. Zhang, L. Fan, Z. Sun, W. Zhang, W. Fan, L. Sun and X. Zhao, *CrystEngComm*, 2013, **15**, 4910; (c) G. Lu, S. Li, Z. Guo, O. K. Farha, B. G. Hauser, X. Qi, Y. Wang, X. Wang, S. Han, X. Liu, J. S. Duchene, H. Zhang, Q. Zhang, X. Chen, J. Ma, S. C. Loo, W. D. Wei, Y. Yang, J. T. Hupp and F. Huo, *Nat. Chem.*, 2012, **4**, 310; (d) Q. Ma, X. Feng, W. Cao, H. Wang and J. Jiang, *CrystEngComm*, 2013, **15**, 10383; (e) W. Cao, H. Wang, X. Wang, H. K. Lee, D. K. P. Ng and J. Jiang, *Inorg. Chem.*, 2012, **51**, 9265.
7. (a) E. D. Bloch, W. L. Queen, R. Krishna, J. M. Zadrozny, C. M. Brown and J. R. Long, *Science*, 2012, **335**, 1606; (b) R. Makiura, S. Motoyama, Y. Umemura, H. Yamanaka, O. Sakata and H. Kitagawa, *Nat. Mater.,* 2010, **9**, 565; (c) S. Horike, Y. Inubushi, T. Hori, T. Fukushima and S. Kitagawa, *Chem. Sci.*, 2012, **3**, 116; (d) J. Kan, H. Wang, W. Sun, W. Cao, J. Tao and J. Jiang, *Inorg. Chem.*, 2013, **52**, 8505; (e) P. Zhu, X. Zhang, H. Wang, Y. Zhang, Y. Bian and J. Jiang, *Inorg. Chem.*, 2012, **51**, 5651.
8. (a) B. Lebeau and P. Innocenzi, *Chem. Soc. Rev.*, 2011, **40**, 886; (b) Y. J. Cui, Y. F. Yue, G. D. Qian and B. L. Chen, *Chem. Rev.*, 2012, **112**, 1126; (c) M. Suh, Y. Cheon and E. Lee, *Coord. Chem. Rev.*, 2008, **252**, 1007; (d) S. T. Meek, J. A. Greathouse and M. D. Allendorf, *Adv. Mater.*, 2011, **23**, 249; (e) C. G. Silva, A. Corma and H. Garcia, *J. Mater. Chem.*, 2010, **20**, 3141.
9. (a) D. C. Zhong, J. H. Deng, X. Z. Luo, H. J. Liu, J. L. Zhong, K. J. Wang and T. B. Lu, *Cryst. Growth Des,* 2012, **12**, 1992; (b) L. B. Sun, Y. Li, Z. Q. Liang, J. H. Yu and R. R. Xu, *Dalton Trans.*, 2012, **41**, 12790; (c) A. Thirumurugan and S. Natarajan, *J. Mater. Chem.*, 2005, **15**, 4588.
10. (a) D.W. Jung, D.A. Yang, J. Kim and W.S. Ahn, *Dalton Trans.*, 2010, **39**, 2883; (b) B. L. Chen, S. Q. Ma, F. Zapata, F. R. Fronczek, E. B. Lobkovsky and H. C. Zhou, *Inorg. Chem.*, 2007, **46**, 1233; (c) B. L. Chen, C. D. Liang, J. Yang, D. S. Contreras, Y. L. Clancy, E. B. Lobkovsky, O. M. Yaghi and S. Dai, *Angew. Chem., Int. Ed.*, 2006, **45**, 1390.
11. (a) M. D. Allendorf, C. A. Bauer, R. K. Bhakta and R. J. T. Houka, *Chem. Soc. Rev.*, 2009, **38**, 1330; (b) J. C. G. Bunzli, *Chem. Rev.*, 2010, **110**, 2729; (c) L. Armelao, S. Quici, F. Barigelletti, G. Accorsi, G. Bottaro, M. Cavazzini and E. Tondello, *Coord. Chem. Rev.*, 2010, **254**, 487; (d) H. B. Xu, X. M. Chen, Q. S. Zhang, L. Y. Zhang and Z. N. Chen. *Chem. Commun.*, 2009, **45**, 7318.
12. (a) F. F. Chen, Z. Q. Chen, Z. Q. Bian and C. H. Huang, *Coord. Chem. Rev.*, 2010, **254**, 991; (b) Y. Ma and Y. Wang, *Coord. Chem. Rev.*, 2010, **254**, 972; (c) J. Rocha, L. D. Carlos, F. A. A. Paz and D. Ananias, *Chem. Soc. Rev.*, 2011, **40**, 926; (d) J. Zhou, Z. Liu and F. Y. Li, *Chem. Soc. Rev.*, 2012, **41**, 1323.
13. (a) C. Marchal, Y. Filinchuk, X. Y. Chen, D. Imbert and M. Mazzanti, *Chem. Eur. J.*, 2009, **15**, 5273; (b) S. L. Huang, Y. J. Lin, W. B. Yu and G. X. Jin, *ChemPlusChem*, 2012, **77**, 141; (c) A. Datcu, N. Roques, V. Jubera, I. Imaz, D. Maspoch, J. Sutter, C. Rovira and J. Veciana, *Chem. Eur. J.*, 2011, **17**, 3644; (d) C. J. Chen, J.Y. Gao, X. Zhao, L. M. Chang, Y. L. Liu, H. H. Mo and S. T. Yue, *Z. Anorg. Allg. Chem.*, 2012, **638**, 2324.
14. (a) G. M. Sheldrick, *SHELXTL*, version 5.1; Bruker Analytical X-ray Instruments Inc.: Madison, WI, 1998. (b) G. M. Sheldrick, *SHELX-97*, PC Version; University of Gottingen: Gottingen, Germany, 1997.
15. (a) V. A. Blatov, A. P. Shevchenko and V. N. Serezhkin, *J. Appl. Crystallogr.*, 2000, **33**, 1193; (b) The network topology was evaluated by the program "TOPOS-4.0", see: http://www.topos.ssu.samara.ru. (c) V. A. Blatov, M. O'Keeffe and D. M. Proserpio, *CrystEngComm*, 2010, **12**, 44; (d) V. A. Blatov, M. O'Keeffe and D. M. Proserpio, *CrystEngComm*, 2010, **10**, 44.
16. (a) A. L. Spek, *J. Appl. Crystallogr.*, 2003, **36**, 7; (b) A. L. Spek, *PLATON, A Multipurpose Crystallographic Tool*, Utrecht University, Utrecht, The Netherlands, 2002.
17. (a) J. H. He, H. Y. Chen, D. R. Xiao, D. Z. Sun, G. J. Zhang, S. W. Yan, G. H. Xin, R. Yuan and E. B. Wang, *CrystEngComm*, 2011, **13**, 4841; (b) D. Sun, F. J. Liu, H. J. Hao, Y. H. Li, N. Zhang, R. B. Huang and L. S. Zheng, *CrystEngComm*, 2011, **13**, 5661; (c) G. Xu and F. Guo, *Inorg. Chem. Commun*, 2013, **27**, 146.
18. (a) K. L. Hou, F. Y. Bai, Y. H. Xing, J. L. Wang and Z. Shi, *CrystEngComm*, 2011, **13**, 3884; (b) K. Chen, D. P. Dong, Z. G. Sun, C. Q. Jiao, C. Li, C. L. Wang, Y. Y. Zhu, Y. Zhao, J. Zhu, S. H.

Sun, M. J. Zheng, H. Tian and W. Chu, *Dalton. Trans*., 2012, **41**, 10948.

19. (a) Y. L. Wang, Y. L. Jiang, Z. J. Xiahou, J. H. Fu and Q. Y. Liu, *Dalton. Trans*., 2012, **41**, 11428; (b) L. Sun, Y. Li, Z. Liang, J. Yu and R. Xu, *Dalton. Trans*., 2012, **41**, 12790.

CrystEngComm

For Table of Contents Use Only

Table of Contents Graphic and Synopsis

Syntheses, Topologies, and Luminescence of Four Ln-Organic Polymers Constructed From Aromatic Tetracarboxylic Acids

Liming Fan, Weiliu Fan, Weikuo Song, Guangzeng Liu, Xiutang Zhang, Xian Zhao

Four interesting Ln coordination polymers based on tetracarboxylate acids have been hydrothermally synthesized through linker extension strategy.